Effective Area of the Cosmic Origins Spectrograph below 1150 Å

Stephan R. McCandliss[1], K. France[2], S. Osterman[2], J. C. Green[2], J. B. McPhate[3], E. Wilkinson[4]
[1]Johns Hopkins University, [2]University of Colorado/Center for Astrophysics and Space Astronomy, [3] University of California/Space Sciences Lab, [4]Southwest Research Institute.
Presented on Wednesday 06 Janurary 2010 in Washington D.C at the 215th Meeting of the American Astronomical Society, Science with the New HST: Cosmic Origins Spectrograph, Poster 464.07

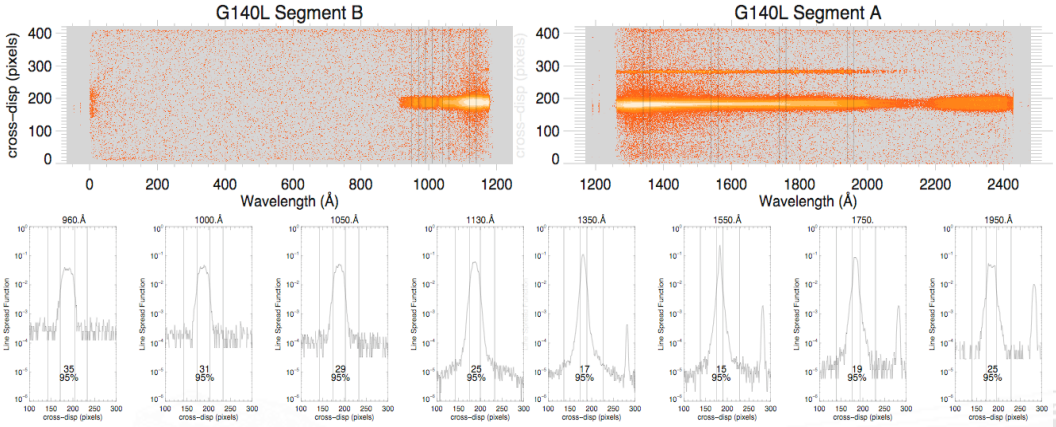

Abstract:

The G140L segment B channel of the Cosmic Origins Spectrograph (COS) recently installed on the *Hubble Space Telescope* (*HST*) has an effective area consistent with ~ 10 cm^2 in the bandpass between the Lyman edge at 912 Å and Ly$_\beta$. It has a slight plateau of ~ 20 cm^2 near 1050 Å and rises to a peak in excess of 1100 cm^2 longward of 1140 Å . This is a new wavelength regime for HST, enabling opportunities for unique science investigations. Investigations seeking to quantify the escape fraction of Lyman continuum photons from galaxies at low redshift, study the He II Gunn-Peterson effect in the redshift range $2 < z < 2.8$, measure CO/H_2 in dense interstellar environments, or make observations of the O VI λλ 1032, 1038 doublet, are now possible. Observations of point sources will have the highest spectral resolution, since the HST point spread function aberrations in the 2."5 diameter COS entrance aperture renders it non-optimal for extended source observations.

Fig 1. -- The G140L segment B and A observations of WD 0320-539 are displayed in the top two panels. The horizontal pixels have been compressed by a factor of ≈ 16 for display purposes. The range of wavelength for each segment is indicated. The vertical dimension is not compressed. The visible detector "footprint" has physical dimensions of ≈ 85 x 10 mm^2. The spectral plate-scale is 13.3 Å mm^{-1} and the angular plate-scale is 3."83 mm^{-1}. Vertical lines in the images indicate the integration regions for the line spread functions (LSF), which are displayed underneath each segment with semi-logarithm scaling. The width, expressed as the number of cross-dispersed pixels, enclosing 95% of the total flux is indicated under each LSF. The astigmatism variation is minimum near 1550 Å. The first spectral order is seen extending from 900 Å to 2100 Å. The second spectral order light can be seen longward of 2100 Å. Some scattered light from zero order is apparent near 0 Å. Scattered light from geo-coronal Lyα in the gap between segments is also apparent.

Overview:

Since the inception of the Cosmic Origins Spectrograph (COS, Morse et al. 1998, Green et al. 2003) it was appreciated that the combination of a single bounce reflection grating with the large geometric collecting area (~40,000 cm^2), and the ~ 15 % reflectivity at 1000 Å of the magnesium fluoride over-coated aluminum (MgF_2/Al) mirrors (Hunter et al. 1971, could provide useful sensitivity in the far-UV bandpass below the MgF_2/Al discontinuity at ~ 1150 Å. This possibility was intriguing because of the potential for new science, such as searching for Lyman continuum leak form star-forming galaxies at low readshift. Moreover, with the loss of *FUSE* the community no longer has access to critical spectral diagnostics, such as for H_2 and OVI, that are only available below 1150 Å.

The COS instrument team found that the windowless detector design and the low resolution G140L grating R (≡ λ/δλ) ~ 2000, lent itself easily to the inclusion of a non-optimized far-UV channel in detector Segment B, spanning ≈ 100 - 1100 Å. Its expected effective area was anticipated to be about 100 to 200 times lower (Froning & Green 2009) than that of COS longward of 1150 Å. However, this estimate was uncertain. It was known that upon return to earth the WFPC-1 pickoff mirror had been severely contaminated during its time on orbit with a normal incidence reflection of ≈ 75% at 1500 Å, falling to ~ 1 % at 1216 (Tveekrem et al.1996). Consequently, the use of the G140L segment B was unsupported for Cycle 17 because of the unknown level of contamination that the *HST* Optical Telescope Assembly (OTA) had suffered in the nearly 20 years since its launch.

Here we present the first evidence that any OTA mirror contamination in the far-UV is inconsequential and that in fact the sensitivity below 1000 Å rivals that of the SiC channels on *FUSE* (Dixon & Kruk 2009). We conclude that "Lyman limited" instrumentation is a feasible option for future large aperture UV telescopes (Moos et al 2004).

Observation:

On 04 September 2009 the hot DA white dwarf WD 0320-539 (T_{eff} = 32.9 K, log g = 7.89, V = 14.9, Vennes et al. 2006) was observed in the G140L channel of COS as part of an external detector flat-field program, number 11491. The spectra for WD 0320-539 were extracted from the two-dimensional Segment B image (Figure 1) using a rectangular aperture 30 pixels high. A detector background region, located at the edge of the detector was similarly extracted. The G140L Segment B wavelength scale is 0.08 Å pixel^{-1} and there are ≈ 6 pixels per spectral resolution element. Spectral pixels are 6 μm wide and cross-dispersion pixels are 24 μm high. Further information on the COS instrument can be found in Green et a. 2010 or in the COS instrument handbook for Cycle 18 (Dixon 2010). This object has also been observed several times by *FUSE,* which provides us with a ready reference for calibration.

Analysis:

In Figure 2 we show the count pixel^{-1} spectrum on a linear scale plotted from 900 -- 1050 Å. The progression of the pressure broadened Lyman series characteristic of a high gravity hot white dwarf is evident. The *FUSE* spectrum is overplotted in blue, demonstrating the effective area is essentially constant in this region. The effective area curve, shown on a semi-logarithmic scale in Figure 3, was derived simply by dividing the FUSE spectrum into the COS count spectrum and scaled to the proper unit. The top panel of Figure 4 is a background spectrum, extracted parallel to the spectral region at the bottom edge of the detector so as to avoid as much as possible light scattered in the cross-dispersion direction. The bottom panel of Figure 4 compares the background to those for the SiC1b, LiF1a and LiF2a channels on FUSE and the He II Gunn-Peterson object HE 2347-4342 (Zheng et al. 2004, Kriss et al. 2001).

References:
Dixon, W. V. & Kruk, J. W. 2009, AIP, 1135, 218–220
Dixon, W. V., ed. 2010, COS Instrument Handbook Cycle 18, Vol 1
Froning, C. S. & Green, J. C. 2009, Ap&SS, 320, 181
Green, J. C., et al. 2010, in preparation
Green, J. C., Wilkinson, E., & Morse, J. A. 2003, SPIE, 4854, 72–80
Hunter, W. R., Osantowski, J. F., & Hass, G. 1971, Appl. Opt., 10, 540
Kriss, G. A., et al. 2001, Science, 293, 1112
Kruk, J. W., Dupuis, J., & Chayer, P. 2009, AIP, 1135, 335–337
Moos, H. W., McCandliss, S. R., & Kruk, J. W. 2004, SPIE, 5488, 1–12
Morse, J. A., et al. 1998, SPIE, 3356, 361–368
Tveekrem, J. L., et al. 1996, SPIE, 2864, 246–257
Vennes, S., Chayer, P., Dupuis, J., & Lanz, T. 2006, ApJ, 652, 1554
Zheng, W., et al. 2004, ApJ, 605, 631

Discussion:

The effective area of COS at wavelengths below 1000 Å is comparable to the effective area of *FUSE* over the same bandpass and it exceeds that of *FUSE* in the 1090 -- 1180 bandpass (Kruk et al. 2009). At present, the error bars at the short wavelength end are somewhat uncertain because of the monotonically decreasing count rate in our calibration object. This situation will improve as further calibrations are acquired. Aside from a small window around 1020 Å, the COS G140L Segment B background limit is smaller that that of *FUSE*, meaning that COS can observe fainter targets in a significantly shorter amount of time longward of 1030 Å and shortward of 1000 Å, albeit at a lower spectral resolution. The combination of reasonable effective area with low detector background will allow COS to pursue science left behind by *FUSE* when the planned low spectral resolution channel was descoped. We estimate that the efficiency of a properly optimized spectrograph on a general purpose 10 meter telescope, having a two bounce OTA with standard MgF_2 /Al mirrors, has the potential to achieve an effective area ~ 500 to 1000 cm^2 in the far-UV.

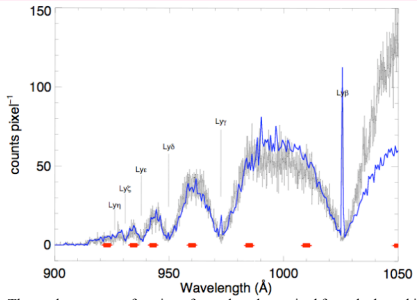

Fig 2. -- The total counts as a function of wavelength acquired from the hot white dwarf WD 0320-539 in 1920 s by the COS G140L Segment B are shown in black. The blue line is the *FUSE* spectrum of the same object multiplied by a constant factor, smoothed and rebinned to the linear wavelength scale of the G140L Segment B. The red points at the bottom of the plot mark the continuum fitting regions.

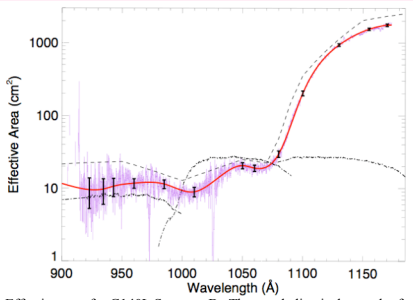

Fig 3. -- Effective area for G140L Segment B. The purple line is the result of dividing the COS spectrum by a *FUSE* spectrum of the same object. The red line is a spline fit to the result. The ± 1σ error bars for the thirteen 3 Å wide wavelength average regions used for the spline fit are shown in black. The dashed line is a model for the effective area based on measured detector, grating and mirror efficiencies. The G140L Segment B effective area ≈ 0.6 times the model near 1000 Å. Effective area curves for the SiC1b, LiF1a and LiF2a channels on *FUSE* (dot-dashed) are shown for comparison.

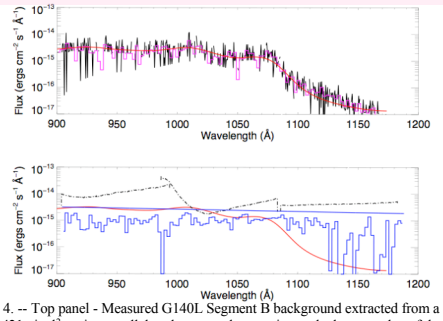

Fig 4. -- Top panel - Measured G140L Segment B background extracted from a 30 X 3421 pixel^2 region parallel to the spectral extraction at the bottom edge of the detector. The black histogram is rebinned from 0.08 Å to 0.48 Å, the purple histogram is rebinned to 2.4 Å. The modeled background is show in red. Bottom panel - Modeled background from *FUSE* (black dot-dashed) are compared to the G140L Segment B background (red). Also included (in blue) are the *FUSE* spectrum of the He II Lyα forest towards HE 2347-4342 rebinned to 2.4 Å and the estimated continuum.